

Springer Series in Advanced Microelectronics 64

Yan Li
Deepak Goyal *Editors*

3D Microelectronic Packaging

From Architectures to Applications

Second Edition

MOREMEDIA



Springer

Springer Series in Advanced Microelectronics

Volume 64

Series Editors

Kukjin Chun, Department of Electrical and Computer Engineering,
Seoul National University, Seoul, Korea (Republic of)

Kiyoo Itoh, Hitachi Ltd., Tokyo, Japan

Thomas H. Lee, Department of Electrical Engineering CIS-205,
Stanford University, Stanford, CA, USA

Rino Micheloni, Torre Sequoia, II piano, PMC-Sierra, Vimercate, MB, Italy

Takayasu Sakurai, The University of Tokyo, Tokyo, Japan

Willy M. C. Sansen, ESAT-MICAS, Katholieke Universiteit Leuven,
Leuven, Belgium

Doris Schmitt-Landsiedel, Lehrstuhl für Technische Elektronik,
Technische Universität München, Munich, Germany

The *Springer Series in Advanced Microelectronics* provides systematic information on all the topics relevant for the design, processing, and manufacturing of microelectronic devices. The books, each prepared by leading researchers or engineers in their fields, cover the basic and advanced aspects of topics such as wafer processing, materials, device design, device technologies, circuit design, VLSI implementation, and sub-system technology. The series forms a bridge between physics and engineering, therefore the volumes will appeal to practicing engineers as well as research scientists.

More information about this series at <http://www.springer.com/series/4076>

Yan Li · Deepak Goyal
Editors

3D Microelectronic Packaging

From Architectures to Applications

Second Edition

 Springer

Editors

Yan Li
Intel Corporation
Chandler, AZ, USA

Deepak Goyal
Intel Corporation
Chandler, AZ, USA

ISSN 1437-0387

ISSN 2197-6643 (electronic)

Springer Series in Advanced Microelectronics

ISBN 978-981-15-7089-6

ISBN 978-981-15-7090-2 (eBook)

<https://doi.org/10.1007/978-981-15-7090-2>

1st edition: © Springer International Publishing Switzerland 2017

2nd edition: © The Editor(s) (if applicable) and The Author(s), under exclusive license to Springer Nature Singapore Pte Ltd. 2021

This work is subject to copyright. All rights are solely and exclusively licensed by the Publisher, whether the whole or part of the material is concerned, specifically the rights of translation, reprinting, reuse of illustrations, recitation, broadcasting, reproduction on microfilms or in any other physical way, and transmission or information storage and retrieval, electronic adaptation, computer software, or by similar or dissimilar methodology now known or hereafter developed.

The use of general descriptive names, registered names, trademarks, service marks, etc. in this publication does not imply, even in the absence of a specific statement, that such names are exempt from the relevant protective laws and regulations and therefore free for general use.

The publisher, the authors and the editors are safe to assume that the advice and information in this book are believed to be true and accurate at the date of publication. Neither the publisher nor the authors or the editors give a warranty, expressed or implied, with respect to the material contained herein or for any errors or omissions that may have been made. The publisher remains neutral with regard to jurisdictional claims in published maps and institutional affiliations.

This Springer imprint is published by the registered company Springer Nature Singapore Pte Ltd.

The registered company address is: 152 Beach Road, #21-01/04 Gateway East, Singapore 189721, Singapore

Contents

1	Introduction to 3D Microelectronic Packaging	1
	Yan Li and Deepak Goyal	
1.1	Introduction	1
1.2	Why 3D Packaging	4
1.2.1	Moore’s Law	4
1.2.2	Small Form Factor Requires 3D Packaging	5
1.2.3	Improved System Performance with Reduced Power	6
1.3	3D Microelectronic Packaging Architectures	7
1.3.1	Die to Die 3D Integration	7
1.3.2	Package to Package 3D Integration	10
1.3.3	Heterogeneous 3D Integration	10
1.4	3D Microelectronic Packaging Challenges	12
1.4.1	Assembly Process, Yield, Test, and Cost Challenges	12
1.4.2	Thermal Management, Package Design, and Modeling Challenges	13
1.4.3	Material and Substrate Challenges	13
1.4.4	Quality, Reliability and Failure Analysis Challenges	14
1.5	Summary	15
	References	15
2	3D Packaging Architectures and Assembly Process Design	17
	Ravi Mahajan and Bob Sankman	
2.1	Introduction	18
2.2	3D TSV Based Architectures: Advantages and Limitations	24
2.3	Methods of Fabrication and Other TSV Attributes	29
2.4	Assembly Process Flows	33

2.5	Manufacturing Yields and the Role of Test	36
2.6	Challenges with 3D TSV Architectures	40
2.7	Summary	40
	References	41
3	Materials and Processing of TSV	47
	Praveen Kumar, Indranath Dutta, Zhiheng Huang, and Paul Conway	
3.1	Introduction	47
3.2	Overview of TSV Materials and Processes	48
3.3	Fabrication of TSV and TSV Assembly	49
	3.3.1 Creating a Via or Trench in Si Wafer	49
	3.3.2 Sequential Filling of Si Via	58
	3.3.3 Planarization and Die-Thinning	61
3.4	Flow Process for Fabricating TSVs and Integration of Dies	63
	3.4.1 Sequence of Flow-Process	63
	3.4.2 Integration of Dies Comprising TSVs	64
3.5	Summary	66
	References	67
4	Microstructure and Mechanical Reliability Issues of TSV	71
	Praveen Kumar, Tae-Kyu Lee, Indranath Dutta, Zhiheng Huang, and Paul Conway	
4.1	Introduction	71
4.2	Microstructural Characterization and Stress Measurement	72
	4.2.1 Microstructural Characterization	72
	4.2.2 Measurement of Stress State	74
4.3	Reliability Issues Associated with TSVs	77
	4.3.1 Stresses in TSVs	77
	4.3.2 Electromigration Related Effects	93
4.4	Towards Atomistically-Informed Reliability Modeling of TSVs	96
	4.4.1 The CPFE Method	96
	4.4.2 The PFC Method	98
4.5	Summary	99
	References	100
5	Phase-Field-Crystal Model: A Tool for Probing Atoms in TSV	107
	Jinxin Liu, Zhiheng Huang, Paul Conway, and Yang Liu	
5.1	Introduction	107
5.2	PFC Model Basics	108
	5.2.1 Classic Density Functional Theory	108
	5.2.2 Model Approximation	110

5.2.3	Model Parameter	114
5.2.4	Governing Equation	117
5.2.5	Extension to Multi-component and Multi-phase Systems	118
5.2.6	Coupling with Physical Field	119
5.3	PFC Model for TSV	123
5.3.1	Triangle Lattice	123
5.3.2	Square Lattice	125
5.3.3	Graphene-Based TSV	126
5.4	Summary	128
	References	128
6	Atomic Scale Kinetics of TSV Protrusion	131
	Jinxin Liu, Zhiheng Huang, Paul Conway, and Yang Liu	
6.1	Introduction	131
6.2	Model Setting and an Example of TSV Protrusion	132
6.3	Protrusion Under Different Mechanical Loading Conditions	135
6.3.1	Shear Strain γ_{yx}	135
6.3.2	Normal Strain ϵ_x and Shear Strain γ_{xy}	135
6.3.3	Normal Strain ϵ_y	137
6.3.4	Loading Distribution	139
6.4	Effect of Grain Structures	143
6.4.1	Grain Distribution	143
6.4.2	Grain Size	145
6.4.3	Grain Orientation	145
6.5	Effect of Temperature	146
6.6	Effect of Geometry	147
6.6.1	TSV Shape	147
6.6.2	Sidewall Roughness	148
6.7	General Perspectives of TSV Protrusion	149
6.7.1	Atomic Mechanisms	149
6.7.2	Prediction Criteria of Protrusion Profile	150
6.7.3	A Viewpoint from Plastic Flow	151
6.8	Future Work	153
	References	154
7	Fundamentals and Failures in Die Preparation for 3D Packaging	157
	Huan Ma, Hualiang Shi, and Erasenthiran Poonjolai	
7.1	Introduction	157
7.2	Brief Overview of TSV Wafer Fabrication Processes	158
7.3	Temporary Wafer Bonding	166
7.4	Wafer Debonding and Clean	169

7.5	Wafer Laser Scribe	178
7.6	Wafer Saw Process	182
7.7	Wafer Die Ejector	186
7.8	Chip Attach	189
7.9	Underfill.	191
7.10	Conclusions	194
	References	194
8	Direct Cu to Cu Bonding and Alternative Bonding Techniques in 3D Packaging	201
	Tadatomo Suga, Ran He, George Vakanas, and Antonio La Manna	
8.1	Introduction	201
8.2	Solder-Based versus Solder-Less Bonding: Pros and Cons	202
8.3	Stacking and Bonding Schemes, Technologies and Applications	204
8.4	Thermo-Compression Bonding (Example of Diffusion Bonding)—Material Fundamentals and Microstructure Effects	206
8.5	Passivation with Capping Layers: Self-assembling Monolayers (SAM's) and Metals	208
8.6	Surface Activated Bonding (SAB) Processes	211
8.7	Cu/Dielectric Hybrid Bonding	215
	8.7.1 Cu/SiO ₂ Hybrid Bonding	216
	8.7.2 Cu/Adhesive Hybrid Bonding	221
8.8	Alternative Cu–Cu Bonding Techniques: Insertion Bonding	223
8.9	Cu–Cu Bonding—Equipment Landscape and State of the Art	225
8.10	Chapter Summary and Recommendations for Future Research	225
	References	226
9	Copper Micro and Nano Particles Mixture for 3D Interconnection Application	233
	Yuanyuan Dai and Chuan Seng Tan	
9.1	Introduction	233
	9.1.1 A Review of Metal Nano-Particles Bonding	233
	9.1.2 Motivation of Mixed Cu Particles Bonding	234
9.2	Packing Density Modeling	235
	9.2.1 Algorithm Design and Assumption	235
	9.2.2 3D Simulation Results	236
	9.2.3 Conclusion	239

- 9.3 Cu Paste Formulation and Characterization 239
 - 9.3.1 Paste Formation and Sintering Profile 240
 - 9.3.2 Thermal and Electrical Characteristics 241
 - 9.3.3 Discussion on Simulation and Experiment Results 248
 - 9.3.4 Summary 249
- 9.4 Demonstration of Die to Wafer Bonding 250
 - 9.4.1 Experimental Details 250
 - 9.4.2 Shear Bond Strength 251
 - 9.4.3 Summary 254
- 9.5 Summary and Outlook 255
 - 9.5.1 Summary 255
 - 9.5.2 Outlook 256
- References 256

10 Fundamentals of Bonding Technology and Process Materials for 2.5/3D Packages 259

Sangil Lee

- 10.1 Introduction 259
- 10.2 Background 260
 - 10.2.1 Overview of 3D Package Configuration 261
 - 10.2.2 Fundamentals of Thermal Compression Bonding (TCB) Technology 264
 - 10.2.3 Fundamentals of Process Materials 274
- 10.3 Principles of Materials Formulation 282
 - 10.3.1 Water Soluble Flux 284
 - 10.3.2 No-Clean Flux 285
 - 10.3.3 Capillary Underfill 286
 - 10.3.4 Epoxy Flux (No-Flow Underfill or Non-conductive Paste) 287
 - 10.3.5 Pre-applied Epoxy Based Materials (Non-conductive Film and B-Stage Material) 289
- 10.4 Assembly Process Design 291
 - 10.4.1 Introduction 291
 - 10.4.2 TCB Assembly Building Block 292
 - 10.4.3 TCB Assembly Building Block Design and Development 294
- 10.5 Special Topic: Comprehensive Comparative Analysis of Microstructure of Sn–Ag–Cu (SAC) Solder Joints by Traditional Reflow and Thermo-Compression Bonding (TCB) Processes 302
 - 10.5.1 Introduction 302
 - 10.5.2 Experimental Section 307
 - 10.5.3 Results and Discussion 312
 - 10.5.4 Conclusion 322

10.6	Summary and Discussion	323
	References	325
11	Fundamentals of Solder Alloys in 3D Packaging	329
	Kwang-Lung Lin	
11.1	The Microbumping Process	329
11.2	The Solder Alloys in Microbump	333
11.3	The Formation of Intermetallic Compounds in the as-Produced Microbump	335
11.4	Microstructure Variation of Microbump Under Thermal Mechanical Conditions	339
11.5	The Microstructure and Failure Mechanism of Microbump	341
11.6	Summary and Future Challenge	342
	References	344
12	Fundamentals of Electromigration in Interconnects of 3D Packaging	347
	Pilin Liu	
12.1	Introduction	347
12.2	Key Modulators for EM in Solder Joints	348
	12.2.1 Typical EM Fail Caused by Sn Diffusion	348
	12.2.2 EM Fail Caused by Metallization Dissolution	351
12.3	EM in Solder Joints of 3D Packaging	355
	12.3.1 EM Damage Due to Sn Flux Divergence in Micro Bumps	355
	12.3.2 The Transformation of Full IMC Joint Under EM	357
	12.3.3 Thermomigration Accompanied by EM	359
12.4	EM in TSV of 3D Packaging	361
	12.4.1 EM for Cu Damascene Interconnects	362
	12.4.2 EM Failure in TSV	363
12.5	Summary	365
	References	366
13	Fundamentals of Heat Dissipation in 3D IC Packaging and Thermal-Aware Design	369
	Satish G. Kandlikar and Amlan Ganguly	
13.1	Introduction	369
13.2	Thermal Performance Parameters for 3D ICs	372
13.3	Air Cooling of 3D ICs	373
13.4	Jet Impingement and Spray Cooling	373
13.5	Microchannel Cooling	374
13.6	Thermal Design Considerations in 3D IC Architectures	375
	13.6.1 Thermal Considerations in TSV Placements	376
	13.6.2 Thermal Analysis Tools for 3D ICs	377
	13.6.3 Performance Considerations	377

13.6.4	Emerging Wireless Interconnects for 3D ICs with Liquid Cooling	378
13.7	Liquid Cooling with Integrated Microchannels	386
13.7.1	Thermal Performance Improvement with Variable Fin Density in Microchannel Passages	387
13.7.2	Two-Phase Cooling	390
13.8	Future Directions	391
	References	392
14	Fundamentals of Advanced Materials and Processes in Organic Substrate Technology	397
	Songhua Shi, Peter Tortorici, Sai Vadlamani, and Prithwish Chatterjee	
14.1	Introduction	397
14.2	Overview of Substrate Technology Evolution	398
14.3	Organic Substrate Materials	399
14.3.1	Materials Employed in Organic Substrate Production	399
14.3.2	General Considerations	400
14.3.3	Substrate and PWB Cores	405
14.3.4	Dielectric Materials	414
14.3.5	PTH and via Filling Materials	416
14.3.6	Solder Mask Materials	417
14.3.7	Surface Finishes	418
14.3.8	Summary	419
14.4	Organic Substrate Fabrication—Process Overview	422
14.4.1	Substrate Raw Material Selection and Preparation	422
14.4.2	Inner Layer Imaging	424
14.4.3	Multi-layer Buildup	424
14.4.4	Soldermask Surface Finish and First Level Interconnect Formation	427
14.4.5	Final Sizing, Testing, Inspection and Shipment	427
	References	428
15	Die and Package Level Thermal and Thermal/Moisture Stresses in 3-D Packaging: Modeling and Characterization	431
	Liangbiao Chen, Tengfei Jiang, and Xuejun Fan	
15.1	Introduction	433
15.2	Thermal Stress and Its Effects on TSV Structures	434
15.2.1	Introduction	434
15.2.2	Characteristics of TSV Stress by Semi-analytic and Numerical Solutions	434

- 15.2.3 Measurement of Thermal Stress 436
- 15.2.4 Effect of Thermal Stress on Carrier Mobility
and Keep-Out Zone 439
- 15.2.5 Thermal Stress Induced via Extrusion 440
- 15.3 Thermal Stresses and the Warpage Control at Package
Level 443
 - 15.3.1 Introduction 443
 - 15.3.2 Thermal Stresses in a Multilayered Structure 444
 - 15.3.3 Warpage Mechanism and Control Methods 446
 - 15.3.4 A Capped-Die Approach for Warpage
Control 448
 - 15.3.5 Warpage Characterization by Experimental
Testing 449
 - 15.3.6 Numerical Modeling for Optimizing Warpage Control
Design 451
- 15.4 Integrated Stress Analysis for Combining Moisture
and Thermal Effects 454
 - 15.4.1 Introduction 454
 - 15.4.2 Moisture Diffusion 455
 - 15.4.3 Moisture-Induced Strain and Effective
Stress Theory 457
 - 15.4.4 Vapor Pressure Modeling 459
 - 15.4.5 Governing Equation for Integrated Stress Analysis 460
 - 15.4.6 Case Studies 461
- 15.5 Summary 465
- References 467

- 16 Processing and Reliability of Solder Interconnections in Stacked
Packaging 471**
Paul Vianco and Mike Nielsen
- 16.1 Introduction 471
 - 16.1.1 Miniaturization and Functionality Trends 471
 - 16.1.2 3-D Packaging Variations 473
 - 16.1.3 Applications Drive PoP and PoPoP Component
Requirements 475
- 16.2 Soldering Assembly Processes 476
 - 16.2.1 Solder Alloys 476
 - 16.2.2 Fluxes and Pastes 479
 - 16.2.3 Assembly Methodologies 481
 - 16.2.4 Inspection Techniques 485
 - 16.2.5 Underfill, Conformal Coatings, and Encapsulants 487
 - 16.2.6 Warpage Effects 491

16.3	Solder Joint Reliability	493
16.3.1	Environments	493
16.3.2	Underfill, Conformal Coatings, and Encapsulants	497
16.3.3	Reliability Studies	499
16.4	Summary and Future Trends	523
16.4.1	Summary	523
16.4.2	Future Trends	523
	References	524
17	Interconnect Quality and Reliability of 3D Packaging	527
	Yaodong Wang, Yingxia Liu, Menglu Li, K. N. Tu, and Luhua Xu	
17.1	Introduction	527
17.2	Quality Challenges for 3D Packaging	528
17.3	Quality and Reliability of Microbumps	533
17.3.1	Type 1—Cu/Sn/Cu	533
17.3.2	Type 2—Ni/Sn/Ni	542
17.3.3	Type 3—Cu/Sn/Ni	544
17.3.4	Type 4—Cu/Ni/Sn/Ni/Cu	546
17.3.5	Concluding Remarks	550
17.4	Field Performance Prediction of 3D Packaging	550
17.5	Electromigration Reliability for 3D IC Packaging	552
17.5.1	Introduction on Electromigration	553
17.5.2	Experimental Studies of Electromigration in Al and Cu Interconnects	555
17.5.3	Electromigration in Flip Chip Solder Joints	556
17.5.4	System Level Electromigration Studies in 3D IC Packaging	557
17.5.5	System Level Weak-Link Failure in 2.5D Integrated Circuits	560
17.5.6	Concluding Remarks	562
17.6	Thermomigration in 3D IC Packaging	562
17.6.1	Introduction	562
17.6.2	Fundamentals of Thermomigration	563
17.6.3	Thermomigration Studies in 3D IC Packaging	565
17.6.4	Concluding Remarks	569
	References	569
18	Fault Isolation and Failure Analysis of 3D Packaging	575
	Yan Li and Deepak Goyal	
18.1	Introduction	575
18.2	Fault Isolation and Failure Analysis Challenges for Advanced 3D Packages	577
18.3	The Application of Non-destructive FI and FA Techniques to 3D Microelectronic Packages	578

- 18.3.1 Non-destructive Fault Isolation Techniques for Electrical Failures in 3D Microelectronic Packages 578
- 18.3.2 High Resolution Non-destructive Imaging Techniques for 3D Microelectronic Packages 586
- 18.4 The Application of Sample Preparation and Material Analysis Techniques to 3D microelectronic packages 600
 - 18.4.1 Sample Preparation Techniques 600
 - 18.4.2 Material Analysis Techniques 602
- 18.5 Failure Analysis Strategies for 3D Packages 607
 - 18.5.1 Understanding the Package Assembly Process, Reliability Stress, and Failure Rate Distribution 607
 - 18.5.2 Efficient FI-FA Flow to Identify Defects 610
 - 18.5.3 In-Depth Failure Mechanism and Root Cause Understanding to Provide Solution Path 612
 - 18.5.4 Conclusions 614
- References 615
- Index 619**

Contributors

Liangbiao Chen ON Semiconductor, 82 Running Hill Rd, South Portland, ME, USA

Paul Conway The Wolfson School of Mechanical, Electrical and Manufacturing Engineering, Loughborough University, Loughborough, Leicestershire, UK

Yuanyuan Dai Nanyang Technological University, Singapore, Singapore

Indranath Dutta School of Mechanical and Materials Engineering, Washington State University, Pullman, WA, USA

Xuejun Fan Department of Mechanical Engineering, Lamar University, Beaumont, TX, USA

Amlan Ganguly Computer Engineering Department, Rochester Institute of Technology, Rochester, NY, USA

Deepak Goyal Intel Corporation, Chandler, AZ, USA

Ran He The University of Tokyo, Tokyo, Japan

Zhiheng Huang School of Materials Science and Engineering, Sun Yat-sen University, Guangzhou, China

Tengfei Jiang Department of Material Science and Engineering, University of Central Florida, Orlando, FL, USA

Satish G. Kandlikar Mechanical Engineering Department, Rochester Institute of Technology, Rochester, NY, USA

Praveen Kumar Department of Materials Engineering, Indian Institute of Science, Bangalore, India

Antonio La Manna IMEC, Louvain, Belgium

Sangil Lee Invensas Corporation, San Jose, CA, USA

Tae-Kyu Lee Department of Mechanical and Materials Engineering, Portland State University, Portland, OR, USA

Menglu Li Department of Materials Science and Engineering, UCLA, Los Angeles, CA, USA

Yan Li Intel Corporation, Chandler, AZ, USA

Kwang-Lung Lin Department of Materials Science and Engineering, National Cheng Kung University, Tainan, Taiwan, ROC

Jinxin Liu School of Materials Science and Engineering, Sun Yat-sen University, Guangzhou, China

Pilin Liu Intel Corporation, Chandler, AZ, USA

Yang Liu School of Electronics and Information Technology, Sun Yat-sen University, Guangzhou, China

Yingxia Liu Department of Materials Science and Engineering, UCLA, Los Angeles, CA, USA

Huan Ma Intel Corporation, Hillsboro, OR, USA

Ravi Mahajan Intel Fellow, High Density Interconnect Pathfinding, Assembly Technology, Intel Corporation, Chandler, AZ, USA

Mike Neilsen Sandia National Laboratories, Albuquerque, NM, USA

Erasenthiran Poonjilai Intel Corporation, Chandler, AZ, USA

Bob Sankman Retired Intel Fellow, High Density Interconnect Pathfinding, Assembly Technology, Intel Corporation, Chandler, AZ, USA

Hualiang Shi Intel Corporation, Chandler, AZ, USA

Songhua Shi Medtronic, Tempe, AZ, USA

Sai Vadlamani Intel Corporation, Chandler, AZ, USA

Tadatomo Suga The University of Tokyo, Tokyo, Japan

Chuan Seng Tan Nanyang Technological University, Singapore, Singapore

Peter Tortorici Medtronic, Tempe, AZ, USA

Prithwish Chatterjee Intel Corporation, Chandler, AZ, USA

K. N. Tu Department of Materials Science and Engineering, UCLA, Los Angeles, CA, USA

George Vakanas Intel Corporation, Santa Clara, CA, USA

Paul Vianco Sandia National Laboratories, Albuquerque, NM, USA

Yaodong Wang Department of Materials Science and Engineering, UCLA, Los Angeles, CA, USA

Luhua Xu Intel Corporation, Chandler, AZ, USA

Chapter 1

Introduction to 3D Microelectronic Packaging



Yan Li and Deepak Goyal

1.1 Introduction

Microelectronic packaging is the bridge between the Integrated Circuit (IC) and the electronic system, which incorporates all technologies used between them [1]. Advanced 3D microelectronic packaging technology is the industry trend to meet portable electronics demand of ultra-thin, ultra-light, high performance with low power consumption. It also opens up a new dimension for the semiconductor industry to maintain Moore's law with a much lower cost [1–3].

A wide variety of real products assembled by the advanced 3D packaging technology have been unveiled in the recent years. For example, the Apple A7 inside the iPhone 5S, introduced in September 2013, is a 3D package with Package on Package (POP) configuration [4]. As displayed in Fig. 1.1, the wire bond Elpida (now Micron) memory (low power double data rate type-3 (LPDDR3) mobile random access memory (RAM)) package is stacked on top of the Apple A7 flip chip package to achieve better performance with smaller form factor. In early 2014, SK Hynix announced its high bandwidth memory (HBM) products having higher bandwidth, less power consumption, and substantially small form factor, achieved by stacking up to eight DRAM dice interconnected through Through Silicon Vias (TSV) and micro bumps [5]. In July of 2015, AMD introduced the AMD Radeon™ Fury graphics cards, the first Graphic Processing Unit (GPU) to implement HBM by TSVs and micro bumps [6]. Figure 1.2 shows a top down and schematic cross sectional view of the advanced 3D package. The big GPU die is integrated into the Si interposer

Y. Li (✉) · D. Goyal
Intel Corporation, Chandler, AZ, USA
e-mail: yan.a.li@intel.com

D. Goyal
e-mail: Deepak.goyal@intel.com

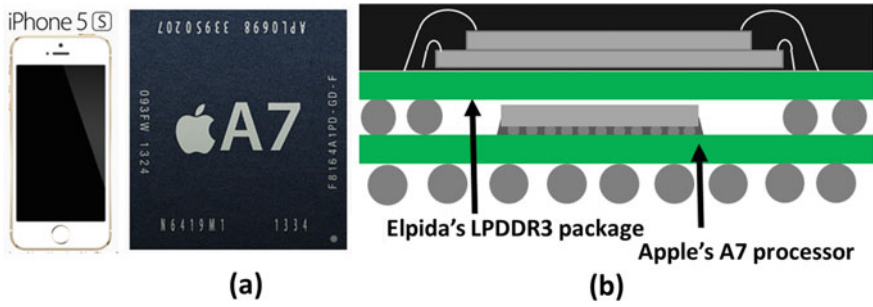


Fig. 1.1 POP inside iPhone 5s. (a) Top view of the Apple A7 package. (b) Schematic of the cross sectional view (not in scale) (Adapted from Ref. [4])

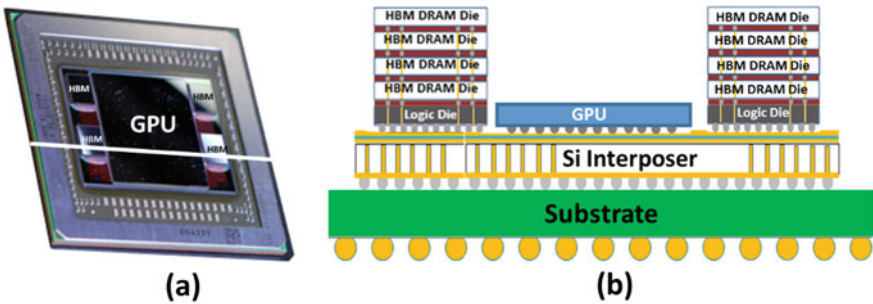


Fig. 1.2 Top view (a) and schematic cross sectional view (not in scale) (b) of the AMD Radeon™ Fury. The big GPU die is integrated into the Si interposer along with four HBM memory stacks by micro bumps and TSVs (Adapted from Ref. [6])

along with four HBM memory stacks by micro bumps and TSVs to ensure faster and shorter connection between chips [6].

Similar packaging technology is called Chip-On-Wafer-On-Substrate (CoWoS) in TSMC, which achieved volume production in 2016, having multiple, advanced chips integrated on a single Si interposer [7].

Since 2018, Intel launched Kaby Lake-G and Stratix 10 series products with the Embedded Multi-Die Interconnect Bridge (EMIB) technology [8]. Instead of using a full silicon interposer, field-programmable gate array (FPGA), transceivers, HBM die stacks, or GPUs in these products connect together through small Si chips embedded in organic substrates and localized high density micro bumps. In 2019, Intel announced Lakefield, the first product using 3D “active interposer” stacking technique called Foveros [9]. The IO, the cores, and the onboard LLC/DRAM can be manufactured as separate dice and get connected together through die stacking 3D packaging technique. The IO die, which is at the bottom of the stack, performs as an “active interposer” that can deal with routing data between the dies on top.

As illustrated in Fig. 1.3, Integrated Fan-Out (InFO) -Package On Package (PoP)

Fig. 1.3 Schematic of Integrated Fan-Out (InFO)—Package on Package (PoP) from TSMC (Adapted from Ref. [10])

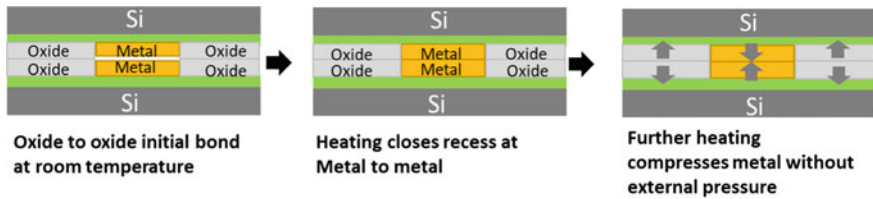
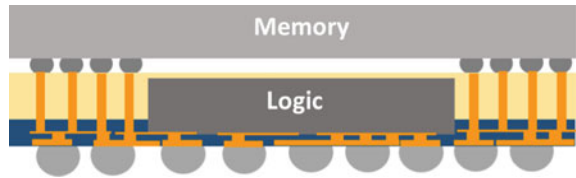


Fig. 1.4 Schematic of Hybrid bonding or Direct Bond Interconnect (DBI) technology from Xperi (Adapted from Ref. [11])

from TSMC, which achieved volume production in 2016, features high density Redistribution Layer (RDL) and Through InFO Via (TIV) to integrate logic die with DRAM package stacking for mobile application [10]. Comparing to Flip Chip PoP, InFO_PoP has a thinner profile and better electrical and thermal performances because of no organic substrate and C4 bump.

Hybrid bonding technology from Xperi, also called Direct Bond Interconnect (DBI), combines a dielectric bond with embedded metal to form interconnect. As demonstrated in Fig. 1.4, the low temperature hybrid bonding solution that allows wafers or die to be bonded with exceptionally fine pitch 3D electrical interconnect enables bump pitch scaling, and has been applied by Sony for 3D stacked back-illuminated image sensors (IMX260) used in Samsung Galaxy S7 Edge in 2016 [11].

These real products bring the 3D packaging techniques from paper to reality, from concept to commercialization, and indicate the extensive applications of 3D packaging technology to microelectronics.

3D packaging technology involves multiple disciplines, for example materials science, mechanical engineering, physics, chemistry, and electrical engineering. A technical book, which could provide a comprehensive scope of 3D microelectronic packaging technology is desirable for graduate students and professionals in both academic and industry area. Current available books on 3D integration typically focus on processing of wafers, especially TSV fabrication, and do not cover other key elements in 3D packaging. This book is proposed to fill in the gap. It presents an thorough extend of 3D packaging, covering the fundamentals of interconnects, bonding process, advanced packaging materials, thermal management, thermal mechanical modeling, architecture design, quality and reliability, and failure analysis of 3D packages, which are critical for the success of advanced 3D packaging.

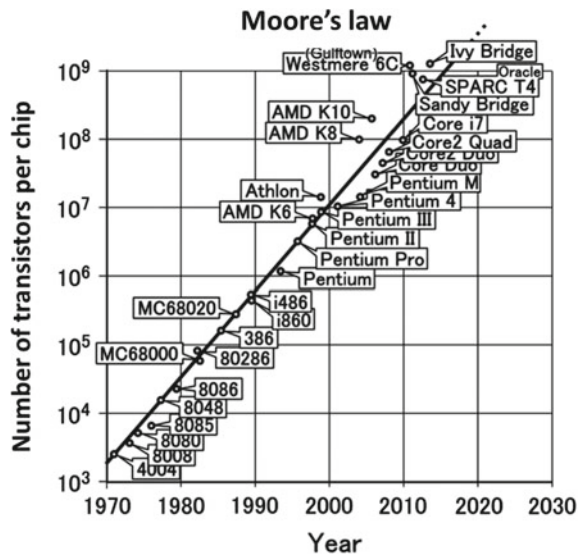
This chapter provides detailed illustration of motivations as well as various architectures of 3D packaging. Challenges in 3D packaging, including fabrication, assembly, cost, design, modeling, thermal management, material, substrate, quality, reliability, and failure analysis, are reviewed with brief introduction to the chapters addressing these challenges.

1.2 Why 3D Packaging

1.2.1 Moore's Law

Since Intel introduced the world's first single-chip microprocessor, the Intel 4004, in 1971, an exponential growth of ICs has been observed following Moore's law in terms of transistor number per chip [12]. As illustrated in Fig. 1.5, the number of transistors per Si chip doubles approximately every 18 months, resulting in a straight line on a log scale [12, 13]. In 1990, the bipolar transistor technology switched to CMOS in order to reduce thermal power, circuit size, and manufacturing costs, at the same time increase the operating speed and energy efficiency [3]. In the early 2000s, multi-core processors were developed to address the challenging thermal power issue in conventional single-core processors [3]. Since multicore processors require enormous cache capacity and memory bandwidth to achieve the designed performance, 3D packaging becomes one of the viable solutions to provide the required cache and bandwidth with a relatively low cost [3].

Fig. 1.5 Moore's law predicts the exponential growth of ICs since 1970s (Adapted from Ref. [13])



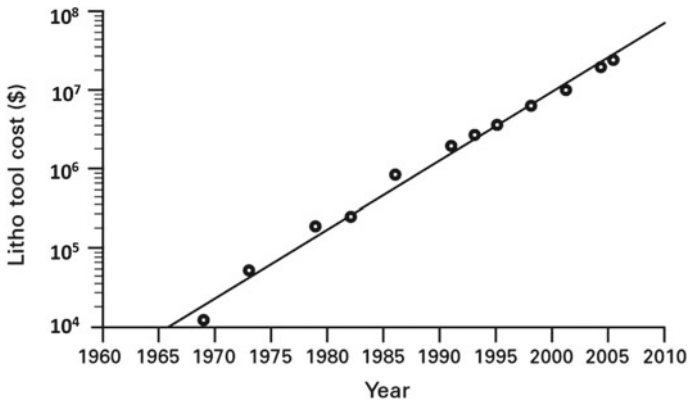


Fig. 1.6 The exponential growth of lithography equipment cost since 1970s (Adapted from Ref. [13])

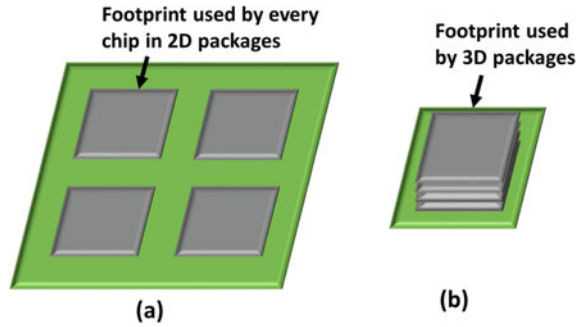
The conventional method to maintain Moore's law is to decrease the dimensions of components by lithography, which is becoming more and more sophisticated and expensive [13]. Figure 1.6 illustrates the exponential growth of lithography equipment cost since 1970s, which presents an economic challenge as the capital cost rises faster than semiconductor industry revenue [13]. 3D integration technology, which has been recognized as an enabling technology for future low cost ICs, provides the third dimension to extend Moore's law to ever higher density, more functionality, better performance with lower cost [3].

1.2.2 Small Form Factor Requires 3D Packaging

Market demands of small form factor microelectronics head to 3D packages, which are ultra-light, ultra-thin, and with small chip footprint. Si chips in 3D packages are typically 50–100 μm thick, about 90% thinner compared with those in conventional packages. Substrate core thickness of 3D packaging is about 0–100 μm , more than 90% thinner than that of traditional packaging. High density interconnects in 3D packaging are on the order of 5–20 μm in diameter, more than 90% smaller than those in 2D packaging. Thus tremendous reduction in size and weight could be achieved by replacing conventional packaging with 3D technology [2].

Small form factor requires small chip footprint, which is defined as the printed circuit board area occupied by the Si chip, as illustrated in Fig. 1.7 [2]. By stacking multiple dice on top of each other using 3D packaging techniques, the chip footprint could be reduced dramatically. Figure 1.7 schematically demonstrates the difference between conventional 2D packages and 3D packages.

Fig. 1.7 a Schematic illustration of the footprint difference between conventional 2D packages (a) and 3D packages (b) (Adapted from Ref. [2])



1.2.3 Improved System Performance with Reduced Power

Interconnect length in 3D packages can be significantly reduced compared with conventional 2D packaging [2]. Figure 1.8a shows a typical interconnect length of 4 mm in a 2D package. The interconnect length could be reduced to 200 μm in a 3D package as demonstrated in Fig. 1.8b. Additionally 3D packaging can also greatly improve the interconnect usability and accessibility [2]. Figure 1.9 shows a comparison between 2D and 3D packaging in terms of the accessibility and usability of interconnection. In contrast to eight neighbors to the center element in the case of 2D packaging technology, the utilization of a 3D packaging configuration provides access to 116 neighbors within an equal interconnect length to a center element in the stack.

The significant decrease in interconnect length as well as dramatic improvement in interconnect usability and accessibility result in much less delay in 3D devices, which is primarily limited by the time taken for the signal to travel along the interconnects [2]. Low latency and wide buses in 3D microelectronic systems lead to significant improvement to the system bandwidth [2]. Noise in well-designed 3D

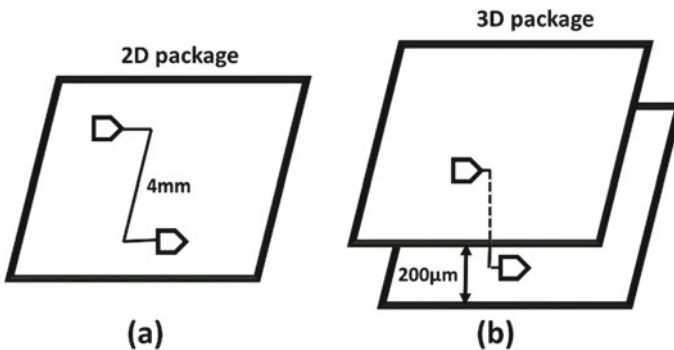


Fig. 1.8 Schematic comparison between the wiring length in 2D packages (a) and 3D packages (b) (Adapted from Ref. [2])

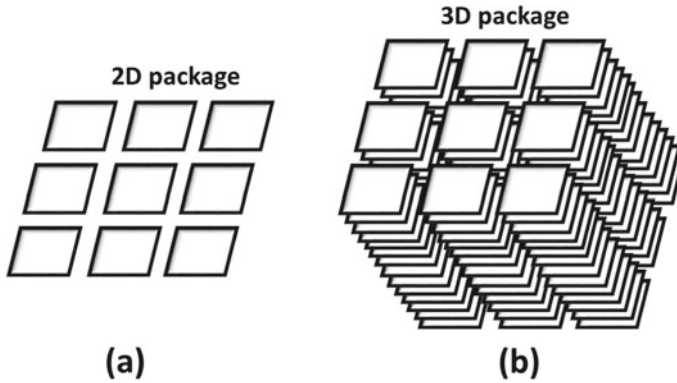


Fig. 1.9 Schematic comparison between 2D packages (a) and 3D packages (b) in terms of the interconnect accessibility and usability (Adapted from Ref. [2])

microelectronic systems, including reflection noise, crosstalk noise, simultaneous switching noise, and electromagnetic interference, can be reduced as a result of the reduction of interconnection length [2]. Additionally, as the parasitic capacitance in microelectronic packages is proportional to the interconnection length, the total power consumption in 3D packages is also reduced because of the reduced parasitic capacitance [2]. The power saving achieved by 3D technology enables 3D devices to perform at a faster rate or transition per second (frequency) with less power consumption. The overall system performance is greatly improved by applying 3D packaging technology [2].

1.3 3D Microelectronic Packaging Architectures

The various 3D packaging architectures could be divided into the following three categories: die to die 3D integration, package to package 3D integration, and heterogeneous 3D integration combining both package and die stacking [3, 14, 15]. Chapter 2 discusses different 3D packaging architectures in detail along with assembly and test flows.

1.3.1 Die to Die 3D Integration

Die to die 3D integration is enabled by through silicon via (TSV) interconnections and thinned die to die bonding [3]. As illustrated in Fig. 1.10, two memory dice are stacked on top of a logic die with TSVs and micro-bumps. First Level Interconnect (FLI) solder joints connects the logic die with the substrate, while Second Level

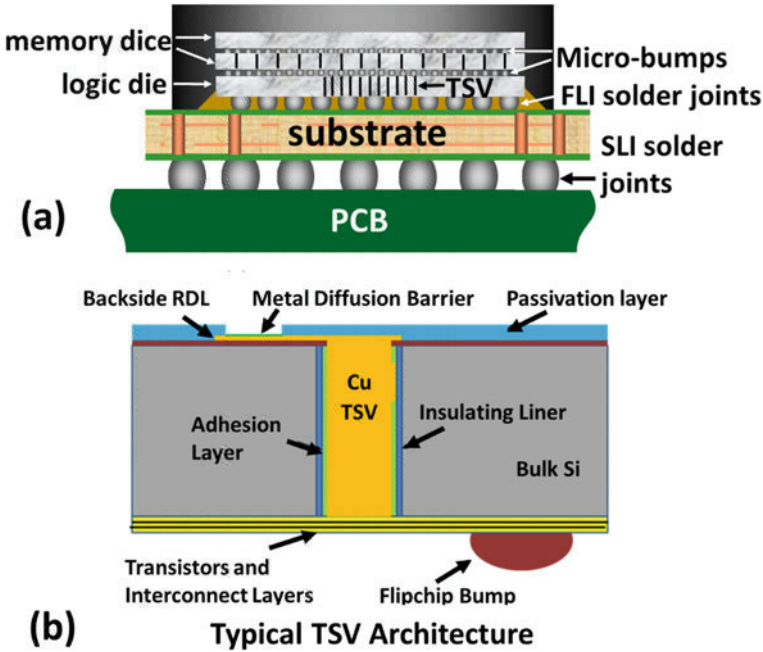


Fig. 1.10 Schematic illustration of die to die 3D integration enabled by TSV and thinned die to die bonding (Adapted from Ref. [15])

Interconnect (SLI) solder joints provides the connection between this 3D package to the Printed Circuit Board (PCB) [15]. The TSVs are formed by laser drilling or deep reactive ion etching, followed by liner deposition and copper fill. There are three typical manufacturing process for TSVs, Via First, Via Middle, and Via Last [16–18]. The detailed process flow of each process as well as the Pros and Cons of each process are discussed in Chaps. 2 and 3.

Die to die bonding is implemented by either Thermal Compression Bonding (TCB) process for solder micro bumps or other alternative bonding process, for example Cu-Cu bonding. Conventional solder mass reflow process in 2D packages, which includes flux dispensing, die attaching, and solder reflow in ovens, is not able to assemble advanced 3D packages having much thinner dice and organic packages, along with much smaller and denser interconnects. As the extend of warpage from both dice and substrates at the reflow temperature overcomes solder surface tension, leading to die misalignment, and results in die tilting, solder joint non-contact opens, and solder bump bridging [19]. TCB bonding process is developed to replace the conventional solder mass reflow process for solder based micro bump assembly in 3D packages. As illustrated schematically in Fig. 1.11, the substrate with pre-applied flux is kept flat on hot pedestal under vacuum to eliminate the substrate warpage. The die is picked up by the bond head, secured and kept flat with vacuum to remove any incoming die warpage. After the die is precisely aligned to the substrate, the

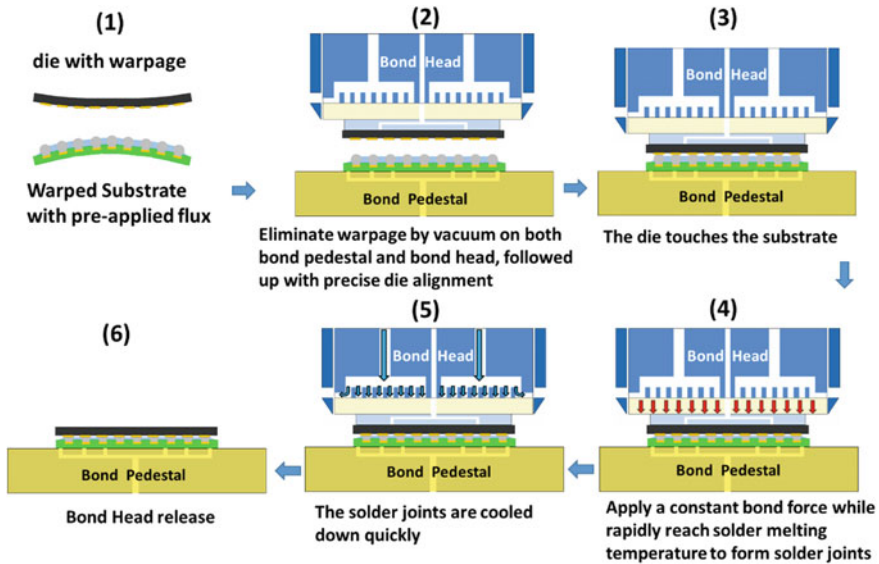
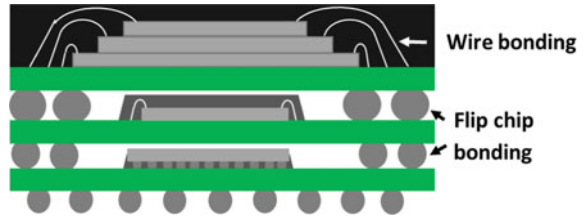


Fig. 1.11 Schematic illustration of a typical Thermal Compression Bonding process (Adapted from Ref. [19])

bond head with die touches the substrate. A constant bond force is then applied on the die through the bond head, while the die is heated up rapidly beyond the solder melting temperature, with a ramping rate higher than $100\text{ }^{\circ}\text{C/s}$. As soon as the solder joints melt, the die is moved further down to ensure all the solder joints are at the same height. The die is held in this position long enough so that the solder joint forms between the die and the substrate. While the solder is still in the molten state, the bond head with die could retract upwards to control the solder joint height. Subsequently, the solder joints are cooled abruptly below the solidus temperature, with a cooling rate of more than $50\text{ }^{\circ}\text{C/s}$, followed up with die release from the bond head [19]. Unlike the traditional solder mass reflow process, with up to 10 min of process time for units in batches, the TCB bonding process assemble units one by one with about a couple of seconds per unit [19]. Additionally, thermal ramping rates during both the heating and cooling cycles are much higher than the conventional method. These higher rates result in solder grain size and orientation differences that can affect mechanical properties as detailed in Chap. 10.

Solder based micro bumps are more compliant, thus could compensate bump height variations, lack of co-planarity, and misalignment issues during high volume manufacture. However the TCB process peak temperature needs to be higher than the melting point of solder material, typically in the range of $250\text{--}300\text{ }^{\circ}\text{C}$, which brings more assembly and reliability challenges. Additionally, solder bridging risk gets much higher as bump pitch shrinks from more than $100\text{ }\mu\text{m}$ to less than $40\text{ }\mu\text{m}$. Alternative bonding process, like hybrid bonding, which could address interconnects with less than $5\text{ }\mu\text{m}$ bump pitch, and assemble at relatively lower temperature is very

Fig. 1.12 Schematic illustration of package to package 3D integration (Adapted from Ref. [3])



promising. Various types of alternative bonding process is reviewed in Chap. 8 as well as Pros and Cons comparing with solder based TCB process.

1.3.2 Package to Package 3D Integration

System in Package (SIP) and Package on Package (POP) are typical configurations of package to package 3D integration, which is enabled by stacking packages through wire bonding or flip-chip bonding [3]. Comparing to die to die stacking, package to package stacking technique has a shorter development cycle, thus help bring products to market faster with a low price. As displayed in Fig. 1.12, a wire bonding package is stacked on top of the other wire bonding package by flip chip bonding. The two packages are then stacked on a flip chip package to form a POP. The conventional solder mass reflow process could still be used in package to package stacking if the package warpages are within control, and the interconnect size and density is comparable with traditional 2D packages. However market demands require packages to be ultra-thin, which limits the number of packages that could be stacked together. Additionally, solder joints and package materials in SIP and POP need to go through multiple cycles of reflow, bringing process and reliability challenges, like solder joint open, delamination between multiple layers in packages, and moisture control between each reflow process. Chapter 17 discusses in detail the processing and reliability of stacked packaging technique, as well as the Pros and Cons comparing with die stacking.

1.3.3 Heterogeneous 3D Integration

Heterogeneous 3D integration assembles separately manufactured components into the same compacted package, thus provides enhanced functionality, lower power consumption, higher system performance, smaller size, and lower costs [9, 20]. Comparing with the monolithic die technology, the heterogeneous 3D integration allows the use of the best available technology node for each chiplet with different functions to maintain maximum performance. It also greatly improves the Si yield due to much smaller die size for each chiplet. The product development cycle can

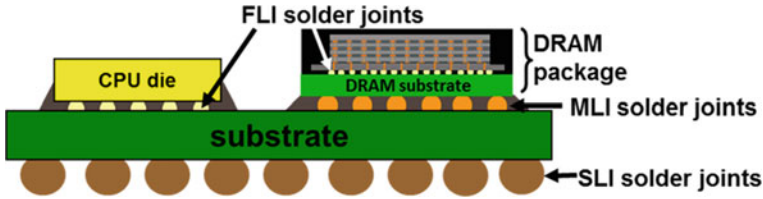


Fig. 1.13 Schematic illustration of 3D packaging architectures having the combination of both die stacking and package stacking (Adapted from Ref. [15])

also be dramatically reduced by integrating commercially available components into the new packages [9, 20].

Depending on product needs, complex heterogeneous 3D packages can have the combination of both die stacking and package stacking [15]. As shown in Fig. 1.13, a 3D Dynamic Random Access Memory (DRAM) package formed by stacking four memory dice on top of the logic die through TSVs and micro bumps is integrated along with a flip CPU chip to form a 3D package by package stacking. FLIs between the CPU chip and the 3D package, MLIs between the DRAM package and the 3D package, as well as interconnects in the substrate provide connection between the CPU chip and the DRAM package [15]. Smaller and denser interconnects between chips and packages are highly desired for better performance, higher bandwidth, and lower power consumption. Figure 1.2 demonstrates the Silicon interposer technology, which could provide better connection between the GPU chip and the HBM die stacks through the Si interposer with dense Cu interconnects and TSVs [15, 21]. Embedded Multi-Die Interconnect Bridge (EMIB) technology is an alternative approach to provide localized high density interconnects between chiplets without Si interposer having TSVs [8]. As illustrated in Fig. 1.14, the link between dice is provided by fine Cu interconnects in Si bridges embedded in the organic substrate and confined denser FLIs between Si bridges and chips. Comparing with Si interposer technology, EMIB technology is able to provide similar performance with

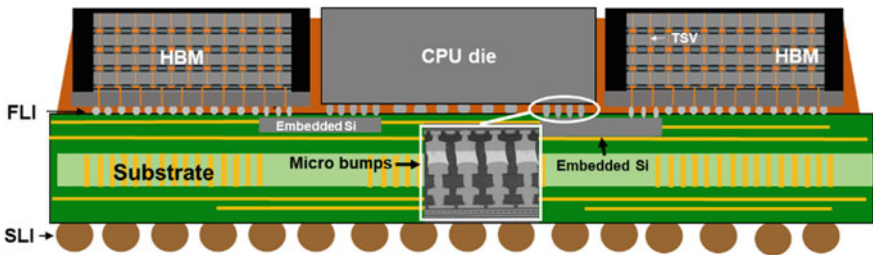


Fig. 1.14 Schematic illustration of Embedded Multi-Die Interconnect Bridge (EMIB) technology providing localized high density interconnects between CPU die and HBM die stacks (Adapted from Ref. [8])

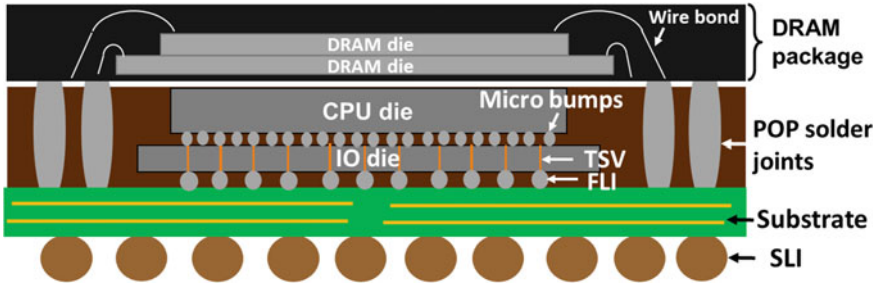


Fig. 1.15 Schematic illustration of a heterogeneous 3D package with Foveros technology providing Face to Face chip stacking between the CPU chip and the IO chip through TSVs and micro bumps. A POP configuration is used to stack a DRAM package to top of the CPU and IO die stack (Adapted from Ref. [9])

a much lower cost, thus opens up new opportunities for heterogeneous 3D packaging [8]. Figure 1.15 illustrates a heterogeneous 3D package for small form factor products, where the package size is constrained. The CPU chip and the IO chip are stacked with Foveros technology, which provides Face to Face connection between chiplets through fine Cu interconnects in chips and micro bumps between chips. TSVs inside the bottom chip are used to connect the organic substrate through FLIs. A POP configuration is used to stack a DRAM package on top of the CPU and IO die stack [9]. The heterogeneous 3D integration approach provides an unprecedented flexibility to chip architects in new product design with various form factor requirements, very aggressive development timeline, better system performance, minimum power consumption, and lowest possible cost.

1.4 3D Microelectronic Packaging Challenges

1.4.1 Assembly Process, Yield, Test, and Cost Challenges

3D packaging involves more challenging assembly steps than conventional packaging, such as TSV wafer fabrication and die singulation process (reviewed in Chap. 7), TCB of micro-bumps (discussed in Chap. 15), multiple solder reflow process for POP (refer to Chap. 17). The complicated process results in yield, test, and cost challenges [2], which could be addressed by redundancy or fault tolerant designs, through-put time (TPT) improvement of assembly process, and minimize process steps based on product quality and reliability requirement [2, 3].